This article was downloaded by: [Institute Of Atmospheric Physics]
On: 09 December 2014, At: 15:18
Publisher: Taylor & Francis
Informa Ltd Registered in England and Wales Registered Number: 1072954 Registered office: Mortimer House, 37-41 Mortimer Street, London W1T 3JH, UK

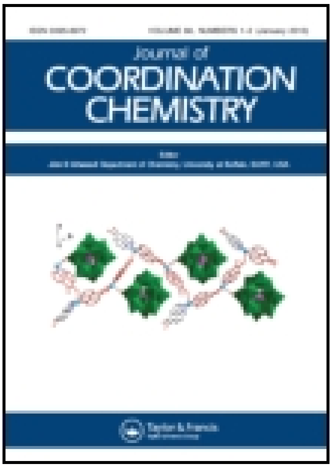

Click for updates

Journal of Coordination Chemistry
Publication details, including instructions for authors and subscription information:
http://www.tandfonline.com/loi/gcoo20

Synthesis, crystal structure, and third-order non-linear optical properties of a new Cd(II) polymer constructed from pyrazine-2-carboxylic acid

Yong Li[a], Wei-Cheng Pan[b], Peng-Zhi Hong[c], Zhao-Xia Zhang[a] & Ke-Chang Li[d]
[a] College of Science, Guangdong Ocean University, Zhanjiang, PR China
[b] College of Chemistry and Food Engineering, Zhongzhou University, Zhengzhou, PR China
[c] College of Food, Guangdong Ocean University, Zhanjiang, PR China
[d] College of Chemistry, Jilin University, Changchun, PR China

Accepted author version posted online: 31 Jul 2014.Published online: 09 Sep 2014.

To cite this article: Yong Li, Wei-Cheng Pan, Peng-Zhi Hong, Zhao-Xia Zhang & Ke-Chang Li (2014) Synthesis, crystal structure, and third-order non-linear optical properties of a new Cd(II) polymer constructed from pyrazine-2-carboxylic acid, Journal of Coordination Chemistry, 67:15, 2630-2642, DOI: 10.1080/00958972.2014.950572

To link to this article: http://dx.doi.org/10.1080/00958972.2014.950572

PLEASE SCROLL DOWN FOR ARTICLE

Taylor & Francis makes every effort to ensure the accuracy of all the information (the "Content") contained in the publications on our platform. However, Taylor & Francis, our agents, and our licensors make no representations or warranties whatsoever as to the accuracy, completeness, or suitability for any purpose of the Content. Any opinions and views expressed in this publication are the opinions and views of the authors, and are not the views of or endorsed by Taylor & Francis. The accuracy of the Content should not be relied upon and should be independently verified with primary sources of information. Taylor and Francis shall not be liable for any losses, actions, claims, proceedings, demands, costs, expenses, damages, and other liabilities whatsoever or howsoever caused arising directly or indirectly in connection with, in relation to or arising out of the use of the Content.

Journal of Coordination Chemistry, 2014
Vol. 67, No. 15, 2630–2642, http://dx.doi.org/10.1080/00958972.2014.950572

Synthesis, crystal structure, and third-order non-linear optical properties of a new Cd(II) polymer constructed from pyrazine-2-carboxylic acid

YONG LI†, WEI-CHENG PAN‡, PENG-ZHI HONG§, ZHAO-XIA ZHANG*† and KE-CHANG LI¶

†College of Science, Guangdong Ocean University, Zhanjiang, PR China
‡College of Chemistry and Food Engineering, Zhongzhou University, Zhengzhou, PR China
§College of Food, Guangdong Ocean University, Zhanjiang, PR China
¶College of Chemistry, Jilin University, Changchun, PR China

(*Received 22 May 2014; accepted 4 July 2014*)

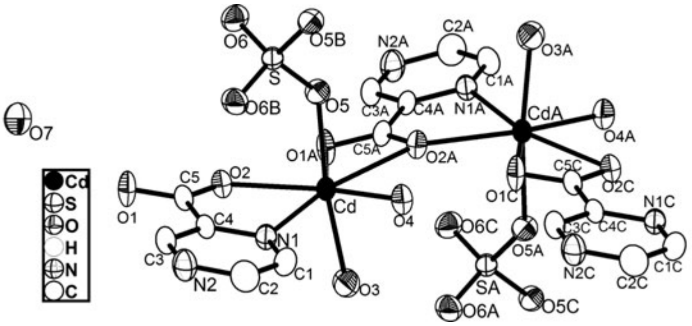

A new cadmium(II) pyrazine-2-carboxylate coordination polymer, $\{[Cd(L)(H_2O)_2(SO_4)_{0.5}]_2{\cdot}H_2O\}_n$ (HL = pyrazine-2-carboxylic acid), has been synthesized by low-temperature solid-state reaction. Single-crystal X-ray analyses reveal that compound possesses a 3-D framework structure. The third-order non-linear optical properties were also investigated and they exhibit nice non-linear absorption and self-defocusing performance with modulus of the hyperpolarizability (γ) 1.30×10^{-30} esu.

A new cadmium(II) pyrazine-2-carboxylate coordination polymer, $\{[Cd(L)(H_2O)_2(SO_4)_{0.5}]_2{\cdot}H_2O\}_n$ (**1**) (HL = pyrazine-2-carboxylic acid), has been synthesized by low-temperature solid-state reaction. Single-crystal X-ray analyses reveal that **1** possesses a 3-D framework structure. The polymer **1** was characterized by elemental analyses, thermogravimetric analyses, X-ray powder diffraction analyses, IR spectra, and UV–visible spectra. The third-order non-linear optical properties were also investigated and they exhibit nice non-linear absorption and self-defocusing performance with modulus of the hyperpolarizability (γ) 1.30×10^{-30} esu for **1** in a 2.01×10^{-4} M dm^{-3} DMF solution.

Keywords: Cadmium(II) compound; Polymer; Structure; Third-order NLO behavior; Synthesis

---

*Corresponding author. Email: yong44176@yeah.net

1. Introduction

Recently, the design and assembly of coordination polymers have been of interest due to their interesting topologies [1–6] and potential applications such as catalysts, superconductors, gas storage, magnetic, and optical materials [7–12]. A rational selection of ligand, metal center, type of the anion, and reaction conditions can confer control over the topology of the resulting networks. Employment of two same metals (such as Cu) or different metals (such as Cu and Cd) [13] in the preparation of coordination polymers may be expected to increase the diversity and complexity of coordination polymers. Many efforts have been devoted to fundamental structural aspects to understand and control the several factors that affect the self-assembly of metal-organic framework architectures. These factors include coordination geometry of metal cations, the structure of organic ligands, the solvent system, pH, temperature, the counter-anion, and the ligand-to-metal ratio [14–20].

The simultaneous presence of sulfate and L^- (pyrazine-2-carboxylic) ligand, which are attractive linkers for crystal engineering, may lead to new polymeric network topologies. L^- has been known to be a versatile ligand, which may coordinate to metal atoms in many different ways [21]. L^- coordinates to metals in O, N coordination, chelating, or bridging. As chelating or bridging ligand, L^- can link a metal center, a pair of metal centers, or many metal centers. In this article, L^- has three kinds of coordination modes to form **1** (see scheme 1).

This compound is synthesized by low-temperature solid-state reaction and not in solution. This low-temperature solid-state synthesis method has significance in reducing environmental pollution. As for non-linear optical (NLO) performance, the studies in the last decade have largely focused on semiconductors, conjugated polymers, and discrete organic molecules [22–25], as well as the fullerene C_{60} [26] while polymers (a very promising class of NLO materials) have been studied to some extent [27] but have not received enough attention. In this article, we report the solid-state synthesis, structural characterization, and the third-order NLO properties of **1**.

2. Experimental

2.1. *Starting materials*

The solvents were carefully dried and distilled prior to use and other chemicals from commercial sources were used without purification.

2.2. *Physical measurements*

Infrared spectra (KBr pellets) were recorded on a Perkin-Elmer SPECTRUM ONE FT-IR spectrometer from 225 to 4000 cm^{-1}. Cd was determined by a Perkin-Elmer Optima 3300DV spectrometer. Elemental analyses (C, H, S, and N) were performed on a

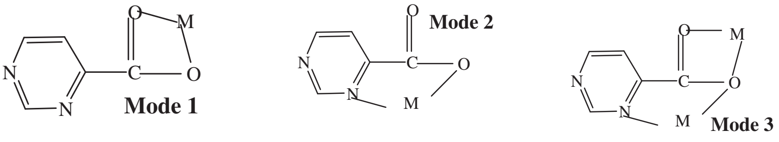

Scheme 1. Three kinds of coordination modes of L^- in **1**.

Perkin-Elmer 2400 Series IICHNS/O elemental analyzer. Electronic spectra were measured on a Shimadzu UV-3100 spectrophotometer. Thermogravimetric analyses were performed on a Perkin-Elmer TGA7 analyzer with a heating rate of 10 °C min^{-1} in a flowing air atmosphere. X-ray powder diffraction (XRPD) intensities were measured on a Rigaku D/max-IIIA diffractometer (Cu Kα radiation, λ = 1.54056 Å) with a scan rate of 1° min^{-1} from 5° to 50°.

2.3. *NLO measurements*

A DMF solution of 2.01×10^{-4} M dm^{-3} of **1** was placed in a 5-mm quartz cuvette for optical measurements. The non-linear absorption and non-linear refraction were measured with a linearly polarized laser light (λ = 532 nm, pulse width = 15 ns) generated from a Q-switched and frequency-doubled Nd–YAG laser. The spatial profiles of the optical pulses were nearly Gaussian. The laser beam was focused with a 25-cm focal-length focusing mirror. The radius of the beam waist was measured to be 30 ± 5 μm (half-width at $1/e^2$ maximum). The incident and transmitted pulse energy were measured simultaneously by two Laser precision detectors (RjP-735 energy probes), which were linked to a computer by an IEEE interface [28]. The interval of each transmittance measurement was set at 5 s, so that every pulse of light was assured of meeting fresh molecules in the sample to eliminate the influence of any photon degradation. The NLO properties of the samples were manifested by moving the samples along the axis of incident beam (*Z*-direction) with respect to the focal point instead of being positioned at its focal point, and an identical setup was adopted in the experiments to measure the *Z*-scan data. An aperture of 0.5 mm radius was placed in front of the detector to assist the measurement of the NLO absorption and refraction effect.

2.4. *Synthesis of 1*

A well-ground mixture of $CdSO_4$ (21 mg, 0.1 mM) and HL (45 mg, 0.1 mM) was heated in a sealed glass tube filled with N_2 gas at 93 °C for 16 h. The mixture was extracted with the mixed solvent of DMF (20 mL), H_2O (5 mL), and CH_3OH (35 mL) and then filtered. The colorless solution filtrate remained in the atmosphere of nitrogen at 5 °C for 6 days and thin colorless crystals were obtained, with yield of 52.0% based on Cd. FT-IR (KBr pellet, cm^{-1}) ν: 3132(w), 2821(w), 2479(w), 2363(w), 1921(m), 1649(w), 1603(s), 1587(s), 1412 (m), 1320(w), 1296(s), 1058(w), 861(w), 779(m), and 685(m). The results of elemental analyses: Anal. Calcd for $C_5H_9O_7N_2S_{0.5}Cd$ (Mr = 337.57): C, 18.28%; N, 8.52%; H, 2.45%; and Cd, 34.21%. Found: C, 18.17%; N, 8.58%; H, 2.55%; and Cd, 34.11%.

2.5. *Structure determination*

A single crystal of **1** was carefully selected under an optical microscope and fixed to a thin glass fiber. Crystal data were collected with graphite-monochromated Mo-Kα radiation (λ = 0.71073 Å) using a Bruker Smart Apex II diffractometer for **1** at T = 296 K. Empirical absorption corrections were made using SADABS [29]. The structures were solved using the direct method and refined by full-matrix least squares on F^2 using the SHELX-97 program package [30]. The non-hydrogen atoms were assigned anisotropic displacement parameters in the refinement; hydrogens were treated using a riding model. The crystal data and selected parameters are given in tables 1 and 2.

Table 1. Crystal data and structure refinement for **1**. Estimated standard deviations are given in parentheses.

Empirical formula	$C_5H_9O_7N_2S_{0.5}Cd$
Formula weight	337.57
Crystal system	Monoclinic
Space group	*C2/c*
Unit cell dimensions	a = 13.768(2) Å, b = 8.4797(14) Å, c = 17.767(3) Å, α = 90.00°, β = 91.977(2)°, γ = 90.00°
Volume (Å^3), Z	2073.0(6), 4
Density (g/cm^3)	1.082
F_{000}	660
Absorption coefficient (mm^{-1})	1.115
Crystal size (mm^3)	0.18 × 0.16 × 0.15
θ range (°)	2.29–25.17
Limiting indices	$-16 \le h \le 14$, $-6 \le k \le 10$, $-17 \le l \le 21$
T (K)	296(2)
Reflections collected/unique	5053/1873 [$R_{(\text{int})}$ = 0.0694]
Data/restraints/parameters	1873/0/165
Goodness of fit indicator	0.928
Final R indicates [$I > 2\sigma(I)$]	R_1 = 0.0309, wR_2 = 0.0637
R indices (all data)	R_1 = 0.0414, wR_2 = 0.0675
Largest diff. peak and hole (e/Å^3)	0.347 and −0.418

Table 2. Selected bond lengths (Å) and angles (°) for **1**. Estimated standard deviations are given in parentheses.

Bond lengths			
Cd–O(2)	2.326(3)	Cd–N(1)	2.429(4)
Cd–O(3)	2.292(4)	S–O(6)	1.452(3)
Cd–O(4)	2.307(4)	S–O(6B)	1.452(3)
Cd–O(5)	2.253(3)	N(1)–C(1)	1.327(6)
S–O(5)	1.488(3)	Cd–O(1A)	2.376(3)
S–O(5B)	1.488(3)	Cd–O(2A)	2.541(3)
Bond angles			
O(5)–Cd–O(3)	171.80(14)	O(5)–Cd–O(4)	85.71(14)
O(5)–Cd–O(2)	87.08(11)	O(3)–Cd–O(4)	92.88(16)
O(5)–Cd–N(1)	97.04(12)	O(3)–Cd–O(2)	98.14(14)
O(4)–Cd–O(2)	148.94(14)	O(3)–Cd–N(1)	90.71(15)
O(4)–Cd–N(1)	80.98(13)	O(2)–Cd–N(1)	69.99(11)
O(6)–S–O(6A)	111.4(3)	O(6)–S–O(5A)	110.34(18)
O(6A)–S–O(5A)	109.89(19)	O(6)–S–O(5)	109.89(18)
O(1A) –Cd–N(1)	146.72(11)	O(6B)–S–O(5B)	109.89(19)

Note: Symmetry transformations used to generate equivalent atoms: A, $-x + 1/2$, $y + 1/2$, $-z + 3/2$; B, $-x + 1$, y, $-z + 3/2$.

3. Results and discussion

3.1. *Synthesis*

The synthesis of **1** could be presumed as follows:

$$2\text{n}\,\text{Cd}^{2+} + 2\text{n}\,\text{L}^{-} + 5\text{n}\,\text{H}_2\text{O} + \text{n}\,\text{SO}_4^{2-} \rightarrow \{[\text{Cd(L)}(\text{H}_2\text{O})_2(\text{SO}_4)_{0.5}]_2 \cdot \text{H}_2\text{O}\}_\text{n}$$

3.2. *Structure description*

The X-ray diffraction analysis reveals that **1** exhibits a 3-D metal–organic framework based on binuclear cadmium building blocks with SO_4^{2-}, L^-, and H_2O ligands. The asymmetric unit of **1** contains one Cd(II), two coordinated waters, two L^- ligands, and one coordinated sulfate. The perspective view of the fundamental unit with the atom-numbering scheme is shown in figure 1. There is one crystallographically unique Cd center in the unit. Cadmium (II) located in the center of a pentagonal bipyramid is seven-coordinated by six oxygens and one nitrogen. The six oxygens are made of three carboxylate groups from two HL ligands (O(2), O(1A), and O(2A)); two oxygens from two waters (O(3) and O(4)); and one oxygen from sulfate (O(5)). The one nitrogen comes from pyrazine of L^- (N(1)). The Cd–O and Cd–N bond distances are comparable to those observed in other complexes [31]. The Cd–O bond lengths range from 2.253(3) to 2.541(3) Å and the O–Cd–O bond angles range from 52.82(12) to 171.80(14)°. Meanwhile, the Cd–N bond lengths are 2.429(4) Å and the O–Cd–N bond angles range from 69.99(11) to 160.45(11)°, as shown in figure 1.

HL in **1** was completely deprotonated, and each L^- bridges two Cd^{2+} ions and adopts μ_2-η^1:η^1:η^1 coordination mode (mode **3**). The μ_2-L^- ligands join the adjacent Cd centers along the *b* direction to a 1-D chain structure $[–Cd-(\mu_2-L)–Cd–]_\infty$, and the μ_2-SO_4^{2-} ligands join adjacent 1-D chain $[–Cd-(\mu_2-L)–Cd–]_\infty$ to a 2-D rhombic-grid network structure $\{[Cd(L)(H_2O)_2(SO_4)_{0.5}]_2{\cdot}H_2O\}_\infty$ along the *ab* plane with 4.718(1) Å and 6.651(4) Å of adjacent Cd···Cd distances formed as shown in figure 2.

Here, Cd(II) ions are regarded as the node; L^- and sulfate as linkers; obviously, the 2-D layer in **1** presents a rhombic topological network. The packing of the molecules of **1** in the solid state exhibits self-assembled structure topologies through different H-bonding and $\pi\cdots\pi$ stacking interactions. The uncoordinated guest H_2O molecules inside these square frameworks are stabilized by hydrogen bonding O–H···O interactions between the sulfate/pyrazine and H_2O of different layers (figure 2), and weak $\pi\cdots\pi$ stacking interactions of 3.554(1) Å (figure 3) resulting in the formation of a 3-D supramolecular packing network (figure 4). The self-assembled structure of the 2-D layer structure further extends to a 3-D supramolecular network, i.e. the individual planes associate with each other through $\pi\cdots\pi$ stacking interactions between the pyrazine rings along the *ac* plane. Interlayer $\pi\cdots\pi$ stacking interaction with the distance of 3.554(1) Å between the centers of two pyrazine rings links

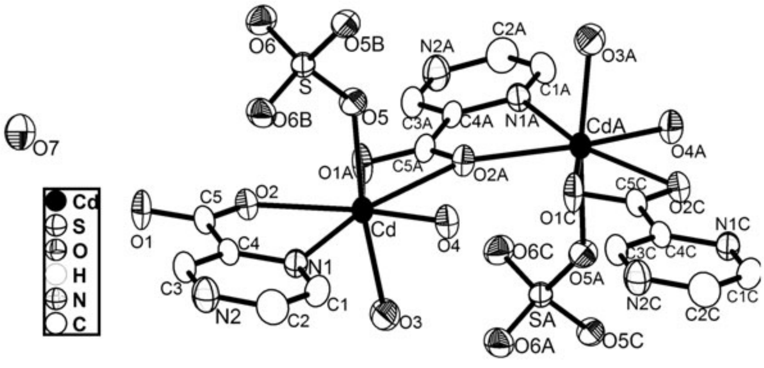

Figure 1. ORTEP view of the building block of **1** with atomic labeling at the 50% probability level. Hydrogens are not shown. Symmetry codes: A, –*x* + 1/2, *y* + 1/2, –*z* + 3/2; B, –*x* + 1, *y*, –*z* + 3/2; C, –*x* + 1/2, *y* – 1/2, –*z* + 3/2.

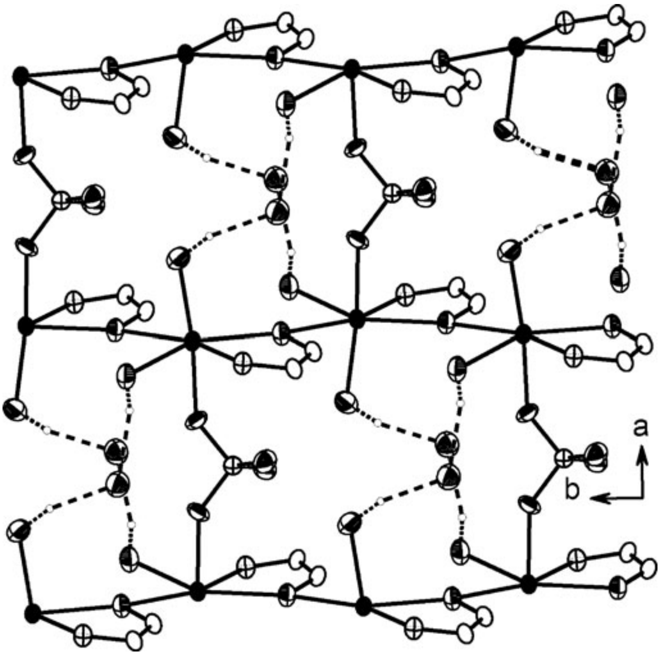

Figure 2. View of the 2-D network structure for **1** along the *ab* plane.

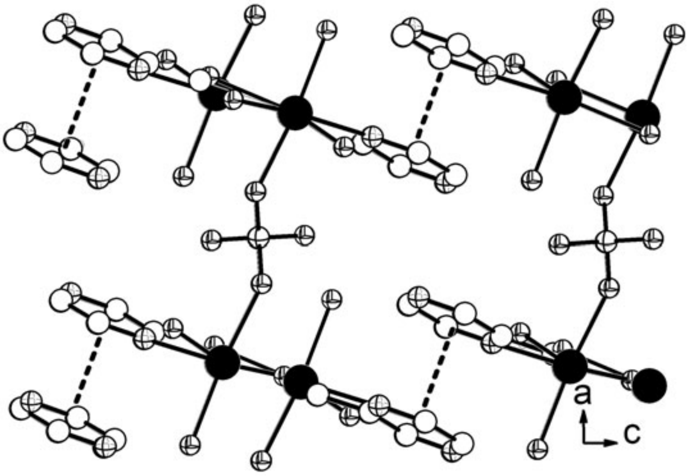

Figure 3. View of the 2-D network structure for **1** along the a*c* plane.

the adjacent coordination layers to form a 3-D network (figure 3). The $\pi\cdots\pi$ distances are comparable to reported [Cu(im)$_2$(NCS)$_2$] (im = imidazole) with $\pi\cdots\pi$ interactions between the imidazole rings (3.783(85) Å) [32].

Supramolecular compounds are one- or poly-dimensional space aggregates with extended structures joined by non-covalent interactions in which hydrogen bonding is the most

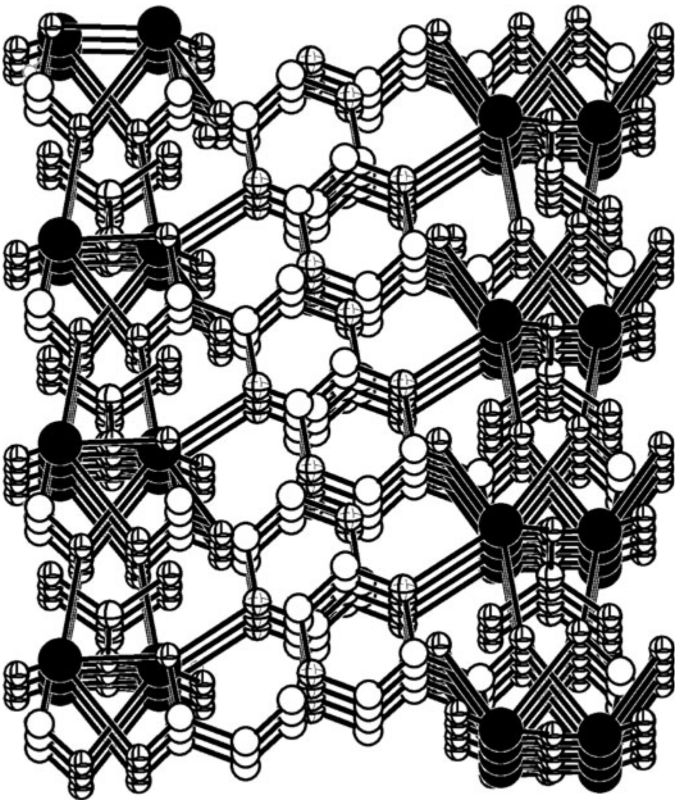

Figure 4. View of the 3-D network structure for **1**.

Table 3. The distances (Å) and angles (°) of hydrogen bonds.

D−H···A	d(D−H)	d(H···A)	d(D···A)	⟨DHA
O(3)−H(3B)···O(7)	0.987(0)	1.855(0)	2.800(0)	159.18(1)
O(4)−H(4B)···O(7)	0.889(0)	1.914(0)	2.782(1)	164.54(1)

dominant intermolecular force. Compound **1** is built up from the 1-D [–Cd-(μ_2-L)–Cd–]$_\infty$ chains, which are connected by μ_2-SO_4^{2-} ligands and two types of hydrogen bond interactions into a 2-D supramolecular network along the *ab* plane. O(7) as acceptor and H(3B) bonding with O(3) H_2O as donor form one type of hydrogen bond O(3)–H(3B)···O(7) [*x*, 1 + *y*, *z*]. On the other hand, O(7) as acceptor and H(4B) bonding with O(4) H_2O as donor form the second type of hydrogen bond O(4)–H(4B)···O(7) [*x*, 1 + *y*, *z*] (figure 2). The two types of hydrogen bonds join the adjacent linear chains along the *ab* plane to form a 2-D network structure. The parameters of all the hydrogen bonds are listed in table 3. The distances of O(3)···O(7) and O(4)···O(7) (2.800(0) Å and 2.782(1) Å, respectively) are within the range of values found for unconventional weak O–H···O hydrogen bonds observed in metal complexes ($d_{O\cdots O}$ = 2.779(27) Å) [33]. As shown in figure 4, a 3-D structure of the neutral polymer was assembled through a combination of coordination bonds, conventional intermolecular O–H···O hydrogen bonds, and weak π–π stacking interactions.

3.3. *NLO properties*

The UV–visible absorption spectrum of **1** (2.01×10^{-4} M dm^{-3} in DMF) displays one strong absorption (with molar absorption coefficients in dm^3 M^{-1} cm^{-1}) at 261 (6.65×10^3) nm and the peak is broad with a long tail of up to 700 nm (figure 5); this is attributed to the ligand centered π–π* transition of L$^-$ and center ion ← ligand charge-transfer transitions. The compound has relatively low linear absorption in the ultraviolet and visible region, and the wide peak extending into the visible region shows the presence of charge-transfer transitions. It also shows that the supramolecular polymer has potential as an optical limiter [34].

The third-order NLO properties of **1** were investigated by using a *Z*-scan technique. The cell being selected to place the sample is a 5-mm-thick glass. The obtained experimental data and theoretical fits [35] are depicted in figure 6. In accordance with the observed effective third-order NLO absorptive coefficient α_2 and refractive coefficient n_2, the modulus of the effective third-order non-linear susceptibility $\chi^{(3)}$ can be calculated by

$$\left|\chi^{(3)}\right| = \left[(9\times10^8 n_0^2\varepsilon_0 c\lambda\alpha_2/8\pi^2)^2 + (n_0 c n_2/80\pi^2)^2\right]^{1/2} \tag{1}$$

where λ is the laser wavelength, n_0 is the linear refractive index of the sample (n_0 can be replaced by one of the solvents during calculation if the concentration of the sample is very dilute), and ε_0 and c are the permittivity and the speed of light in a vacuum, respectively. The corresponding modulus of the third-order non-linear molecular susceptibilities (or hyperpolarizabilities) was obtained from

$$|\gamma| = |\chi^{(3)}|/\mathrm{NF}^4 \tag{2}$$

where $F^4 = [(n^2 + 2)/3]^4$, N is the molecular number density of the compound in the sample (i.e. molecular number of the solute in each mL of the solution), and F^4 is the local Lorents

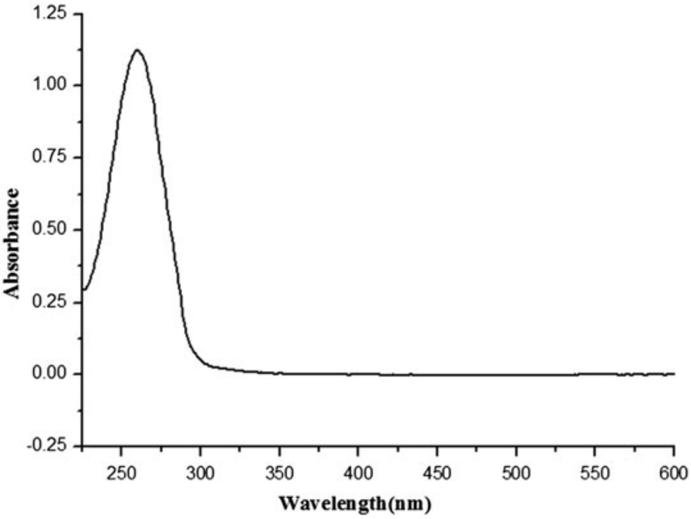

Figure 5. UV–visible spectrum of **1**.

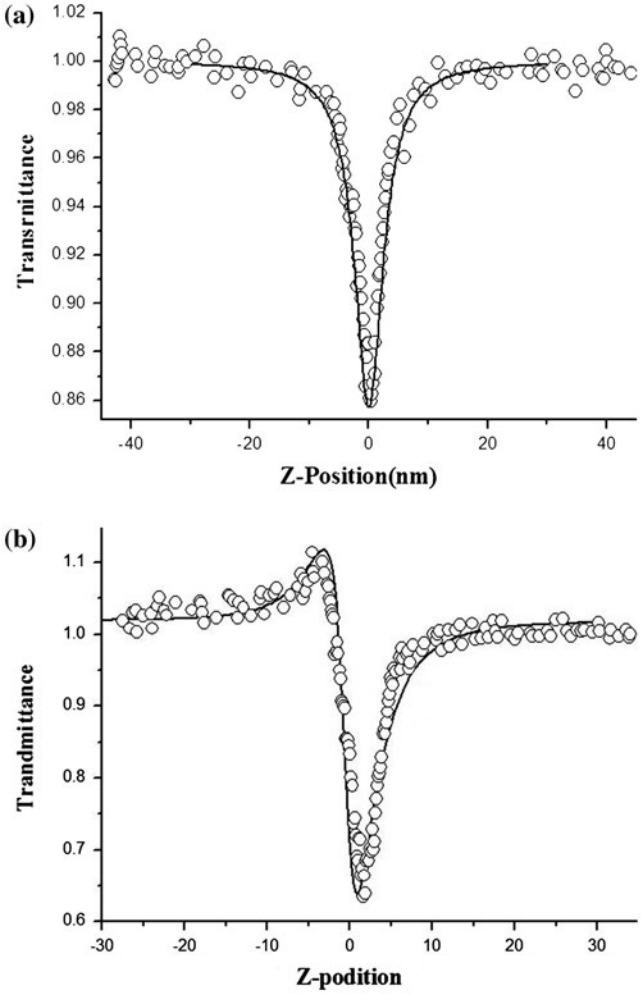

Figure 6. *Z*-scan data of **1** dissolved in DMF with a concentration of 2.10×10^{-4} M dm^{-3}. The circles represent experimental data and the solid curve is a theoretical fit. The data were collected under an open (a) or closed (b) aperture configuration showing NLO absorption.

field correction term. All the calculated results and some literature data on the NLO properties are listed in table 4. The γ value in the table indicates that **1** has nicer third-order NLO performance and displays the reverse saturation absorption ($\alpha_2 > 0$) and a self-defocusing property ($n_2 < 0$). The material possessing the self-defocusing performance may be an excellent one for application in protection of optical sensors.

Supramolecular **1** exhibits a significant NLO absorption and a refractive effect. The hyperpolarizability γ value (1.30×10^{-30} esu) of **1** is comparable to that of [Co(ISO-IN)$_2$(H$_2$O)$_4$] (**2**) (8.75×10^{-31} esu) [33] and [Co(im)$_2$(C$_2$O$_4$)] (**3**) (1.55×10^{-31} esu) [36]. The third-order NLO properties of some compounds are listed in table 4. The three compounds possess a similar supramolecular structure, but center ions and external ligands are different. As a result, the three compounds exhibit self-defocusing effects ($n_2 < 0$) and

Table 4. Third-order NLO properties of some compounds.

Compounds	Concentrations (M dm^{-3})	α_2 (m/w)	n_2 (m^2/w)	$\chi^{(3)}$ (esu)	γ (esu)	Ref.
$\{[Cd(L)(H_2O)_2]_2SO_4\cdot H_2O\}_n$ (**1**)	2.01×10^{-4}	1.62×10^{-11}	-5.37×10^{-19}	8.03×10^{-12}	1.30×10^{-30}	This work
$[Co(ISOIN)_2(H_2O)_4]$ (**2**)	1.56×10^{-4}	1.15×10^{-11}	-5.12×10^{-19}	7.82×10^{-12}	8.75×10^{-31}	[33]
$[Co(im)_2(C_2O_4)]$ (**3**)	1.40×10^{-3}	0.82×10^{-11}	-4.30×10^{-19}	4.30×10^{-13}	1.55×10^{-31}	[36]

Note: HL = pyrazine-2-carboxylic acid; H_2ISOIN = isonicotinic acid; im = imidazole.

effective n_2 values are -5.37×10^{-19} $m^2 W^{-1}$ for **1**, -5.12×10^{-19} $m^2 W^{-1}$ for **2**, and -4.30×10^{-19} $m^2 W^{-1}$ for **3**. This is consistent with the fact that center metal and peripheral ligand substitution induce larger changes in the NLO properties as observed in supramolecular compounds. As for the interrelation between structure and optical performance, we can attribute the nicer NLO properties of these compounds to the presence of large delocalized electron cloud in the supramolecular compounds. This very fact strongly implies that the compounds may be designed and synthesized to obtain good NLO materials. Further work on our research in this field is in progress.

3.4. *Thermogravimetric analysis*

Thermal stability of the complexes was investigated by TGA (figure 7). The thermal behavior of the Cd(II) polymer **1** was followed up to 700 °C in flowing air with a heating rate of

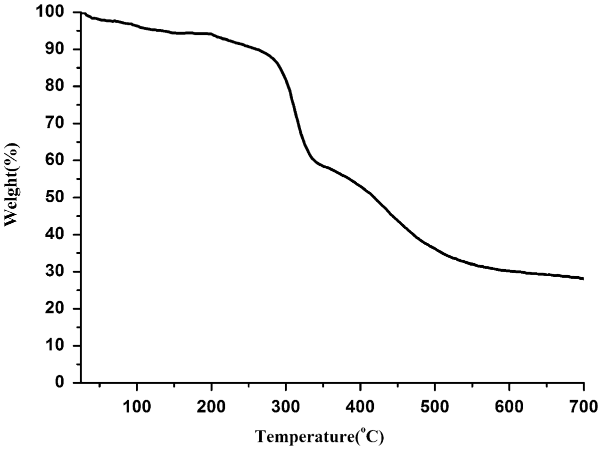

Figure 7. Thermogravimetric patterns for **1**.

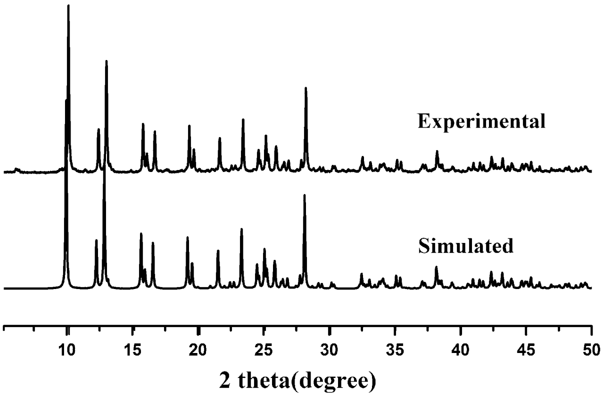

Figure 8. Experimental and simulated X-ray diffraction patterns of **1**.

10 °C min^{-1}. Thermal analysis of the polymer shows that it decomposes in three steps. In the first step, the TGA curve of **1** shows weight loss of 2.45% around 105 °C from removal of crystal waters at apical positions (Calcd 2.67%). In the second step, weight loss of 5.40% from 105 to 279 °C is due to the removal of coordinated water (Calcd 5.33%). Then, the framework begins to decompose when the temperature rises to 279 °C. In the third step, the ligands of **1** are lost. The experimental mass loss is in agreement with the theoretical mass loss in all the steps.

3.5. *XRPD analysis*

Figure 8 shows the experimental and simulated powder X-ray diffraction patterns of **1**, which are in agreement with each other, suggesting the phase purity of the as-synthesized product.

4. Conclusion

A new Cd(II) 3-D metal–organic polymer with mixed connectors of SO_4^{2-}, L^-, and H_2O has been low-temperature synthesized. No Cd complexes with this kind of three ligands linking mode are known. The polymer exhibits good third-order NLO absorption and self-defocusing performance in DMF solution. Both effects will offer a thought for design and synthesis of optical materials.

Supplementary material

Supplementary material have been deposited with the Cambridge Crystallographic Center, CCDC No. 995630 for **1**. Copy of this information may be obtained free of charge from The Director, CCDC, 12, Union Road, Cambridge CB2 1EZ, UK. (Fax: +44-1223-336033; E-mail: deposit@ccdc.cam.ac.uk or www: http://www.ccdc.cam.ac.uk).

Funding

This research was supported by grants from the Guangdong Ocean University Science Foundation of China [grant number C13435].

References

[1] P.J. Hagrman, D. Hagrman, J. Zubieta. *Angew. Chem. Int. Ed.*, **38**, 2639 (1999).
[2] Y.B. Dong, M.D. Smith, R.C. Layland, H.C.Z. Loye. *Chem. Mater.*, **12**, 1156 (2000).
[3] I.A. Ibarra, T.W. Hesterberg, B.J. Holliday, V.M. Lynch, S.M. Humphrey. *Dalton Trans.*, **41**, 8003 (2012).
[4] Y. Li, Z.-X. Zhang, Q.-S. Li, W.-D. Song, K.-C. Li, J.-Q. Xu, Y.-L. Miao, L.-Y. Pan. *J. Coord. Chem.*, **60**, 795 (2007).
[5] X. Lin, A.J. Blake, C. Wilson, X.Z. Sun, N.R. Champness, M.W. George, P. Hubberstey, R. Mokaya, M. Schroeder. *J. Am. Chem. Soc.*, **128**, 10745 (2006).
[6] J. Albanez, I. Brito, A. Cárdenas, M. López-Rodríguez. *Acta Crystallogr., Sect. E: Struct. Rep. Online*, **67**, m1339 (2011).
[7] H. Furukawa, K.E. Cordova, M. Okeeffe, O.M. Yaghi. *Science*, **341**, 1230444-1 (2013).
[8] X.X. Xu, X.X. Liu, X.G. Sang, E.B. Wang. *J. Coord. Chem.*, **63**, 3060 (2010).
[9] N.B. Shustova, A.F. Cozzolino, S. Reineke, M. Baldo, M. Dinca. *J. Am. Chem. Soc.*, **135**, 13326 (2013).
[10] J.R. Li, R.J. Kuppler, H.C. Zhou. *Chem. Soc. Rev.*, **38**, 1477 (2009).
[11] J.W. Cheng, J. Zhang, S.T. Zheng, M.B. Zhang, G.Y. Yang. *Angew. Chem. Int. Ed.*, **45**, 73 (2006).
[12] N.W. Ockwig, O. Delgado-Friederichs, M. O'Keeffee, O.M. Yaghi. *Acc. Chem. Res.*, **38**, 176 (2005).

[13] Y. Li, Z.-X. Zhang, K.-C. Li, W.-D. Song, Q.-S. Li. *Inorg. Chem. Commun.*, **10**, 1557 (2007).
[14] D.M. Shin, I.S. Lee, Y.A. Lee, Y.K. Chung. *Inorg. Chem.*, **42**, 2977 (2003).
[15] G. Liu. *Acta Crystallogr., Sect. E: Struct. Rep. Online*, **66**, m93 (2010).
[16] R.Q. Fang, X.M. Zhang. *Inorg. Chem.*, **45**, 4801 (2006).
[17] Y.B. Dong, Y.Y. Jiang, J. Li, J.P. Ma, F.L. Liu, B. Tang, R.Q. Huang, S.R.J. Batten. *J. Am. Chem. Soc.*, **129**, 4520 (2007).
[18] P. Zhang, E.B. Wang, C.Y. Xing, P.L. Kang, K. Li. *Chin. J. Inorg. Chem.*, **25**, 560 (2009).
[19] R.W. Saalfrank, I. Bernt, M.M. Chowdhry, F. Hampel, G.B.M. Vaughan. *Chem. Eur. J.*, **7**, 2765 (2001).
[20] N.L. Toh, M. Nagarathinam, J.J. Vittal. *Angew. Chem. Int. Ed.*, **44**, 2237 (2005).
[21] T. Matsuda, J. Kim, Y. Moritomo. *J. Am. Chem. Soc.*, **132**, 12206 (2010).
[22] M. Samoc, A. Samoc, B.L. Davies, M.G. Humphrey, M.S. Wong. *Opt. Mater.*, **21**, 485 (2003).
[23] A.R. Dias, M.H. Garcia, J.C. Rodrigues, J. Petersen, T. Bjornholm, T. Geisler. *J. Mater. Chem.*, **5**, 1861 (1995).
[24] H. Huang (Ed.). *Optical Nonlinearities and Instabilities in Semiconductors*, Academic Press, New York (1988).
[25] C. Ornelas, C. Gandum, J. Mesquita, J. Rodrigues, M.H. Garcia, N. Lopes, M.P. Robalo, K. Nattinen, K. Rissanen. *Inorg. Chim. Acta*, **358**, 2482 (2005).
[26] Y.P. Sun, J.E. Riggs. *Int. Rev. Phys. Chem.*, **18**, 43 (1999).
[27] Y. Li, Z.X. Zhang, F.Y. Fang, W.D. Song, K.C. Li, Y.L. Miao, C.S. Gu, L.Y. Pan. *J. Mol. Struct.*, **837**, 269 (2007).
[28] M.A.S. Goher, F.A. Mautner. *Polyhedron*, **18**, 2339 (1999).
[29] G.M. Sheldrick. *SADABS Program for Scaling and Correction of Area Detector Data*, University of Göttingen, Göttingen (1996).
[30] (a) G.M. Sheldrick. *SHELXL-97, Programfor X-ray Crystal Structure Refinement*, University of Göttingen, Göttingen (1997); (b) Bruker, *APEXII software, Version 6.3.1*, Bruker AXS Inc., Madison, WI (2004).
[31] S.G. Lee, K.M. Park, Y. Habata, S.S. Lee. *Inorg. Chem.*, **52**, 8416 (2013).
[32] H.Y. Bie, J.H. Yu, J.Q. Xu, J. Lu, Y. Li, X.B. Cui, X. Zhang, Y.H. Sun, L.Y. Pan. *J. Mol. Struct.*, **660**, 107 (2003).
[33] Y. Li, Z.X. Zhang, Z.X. Wu, K.C. Li, Q.S. Li. *Polish J. Chem.*, **83**, 373 (2009).
[34] C. Zhang, Y.L. Song, F.E. Kuhn, Y. Xu, X.Q. Xin, H.K. Fun, W.A. Herrmann. *Eur. J. Inorg. Chem.*, **1**, 55, (2002).
[35] A. Müller, H. Bogge, U. Schimanski. *Inorg. Chim. Acta*, **69**, 5 (1983).
[36] J.H. Yu, J.Q. Xu, L.J. Zhang, J. Lu, X. Zhang, H.Y. Bie. *J. Mol. Struct.*, **743**, 243 (2005).